Effect of magnetic Gd adatoms on the transport properties of ultrathin gold films

M. Alemani,* A. Huegel, E. Helgren,† D. R. Queen, and F. Hellman
Department of Physics, University of California–Berkeley, Berkeley, California 94720, USA
(Received 27 January 2010; revised manuscript received 7 September 2010; published 30 November 2010)

Ultrathin two-dimensional gold films have been grown on an amorphous Ge underlayer by quench condensation at low temperature, followed by adsorption of magnetic Gd atoms and nonmagnetic Y atoms. The resulting electrical transport as a function of temperature and composition has been investigated *in situ*. Gold films of different sheet resistances ($R_{\square}$) have been used for the Gd and Y adsorption platform. The temperature and thickness dependence of the conductance G ($G=1/R_{\square}$) indicates that the Au films cross from a strongly localized regime, where conductivity is through hopping and where electron correlation effects are expected to be strong, to a weakly localized regime. The system is shown to be sensitive to different added electronic states, in that adding Gd or Y increases G, but much less than adding the same amount of Au for all initial G values. No difference is observed (down to 5 K) between added Gd and Y, showing that there is no effect of the Gd magnetic moments on electrical transport. The absence of magnetic localization and dominance of adding electronic states over added electronic potential disorder in this quench-condensed ultrathin system is discussed and attributed to the intrinsically high electronic concentration of Au.

DOI: 10.1103/PhysRevB.82.195447 PACS number(s): 73.20.Hb, 75.70.−i, 73.63.−b, 71.23.−k

Chemical doping is a well-known and widely used method to manipulate the electronic properties of materials. By adding dopants to a semiconducting system, it is possible to increase conductivity, producing a zero-temperature ($T=0$ K) metal-insulator-transition (MIT) as a function of doping concentration x. Nonmagnetic dopants atoms produce small magnetoresistance (MR) values of both signs[1] whereas magnetic atoms used as dopants can lead to extremely large negative MR values[2] due to interactions between conduction electrons and local magnetic moments of the dopants.[3,4] For example, transport measurements on three-dimensional (3D) *a*-Gd-Si show strong localization of carriers caused by the Gd local moments and many orders of magnitude negative MR.[5] In the absence of a magnetic field, the Gd spin is randomly oriented and thus adds an additional disorder compared to nonmagnetic Y-doped analog systems, leading to strong suppression of conductivity below a characteristic temperature.[5,6] With increasing field the Gd spins align, thus reducing the disorder in the system and increasing the conductivity. These effects are enhanced near the MIT, where localization due to disorder and electron correlations effects become crucial.

We are here interested in studying the effects of Gd magnetic disorder on transport of a highly disordered two-dimensional (2D) system since electron correlation and disorder effects are known to be strong in 2D (Refs. 7 and 8) and large negative MR and enhanced localization might be expected by analogy to the 3D results near the MIT described above. Magnetic impurities on surfaces have been intensively studied in the weak disorder regime,[9] where their effect on transport has been explained by means of weak localization, and inelastic, spin-orbit, and magnetic scattering times have been determined.[10,11] However, very little has been explored with *f*-state impurities such as due to Gd, or for any magnetic impurities in the strong disorder regime.

We have grown ultrathin Au films on a Ge-coated substrate at cryogenic temperature, which form the simplest realization of a quasi-2D disordered electron system. We have measured the dc conductance of these Au films on adding submonolayer quantities of either magnetic Gd or nonmagnetic Y adatoms. Gd is a $4f^7 5d^1 6s^2$ atom, virtually always trivalent in the solid state, resulting in $J=S=7/2$ and $L=0$ due to the half filled *f* shell, and no magnetic anisotropy. Y ($4d^1 5s^2$), as Gd, is a trivalent material with nearly identical ionic radius as Gd. Therefore, Y and Gd should introduce the same electronic potential disorder to the system and similar outermost electrons, hence carriers. They differ only by the presence or absence of the inner $4f$ shell of Gd, which at least in 3D semiconducting materials causes magnetic disorder which strongly impacts electrical conduction and creates enormous (negative) magnetoresistance, as discussed above.

The films were grown by sequential evaporation of Ge, Au and either Gd or Y onto a substrate held at cryogenic temperature while monitoring film thickness t and conductance G in an ultrahigh-vacuum chamber with base pressure in the low 10^{-9}–10^{-10} Torr regime. The temperature of the substrate during subsequent measurement was kept lower than 15 K because irreversible changes in G, due most probably to structural changes/crystallization of the Au films, were seen above 20 K.

Films were grown on amorphous SiN_x- and SiO_x-coated Si substrates with prepatterned electrical leads. Prior to the Au deposition, a 10 Å wetting layer of Ge was deposited on the substrate. Substrates with or without Ge show measured resistance greater than 10^{11} Ω. It is well established that this Ge underlayer causes the metallic layer to grow more uniformly, giving a measurable electrical conductivity for thickness of a few (1–2) monolayers (MLs).[12,13] By contrast, thin Au films quench-condensed directly on, e.g., fire-polished glass, are nonuniform, consisting of disconnected islands.[14] Scanning tunneling microscopy measurements show that Au films grown at low temperature (77 K) on Ge underlayers are structurally disordered (amorphous) and uniform in thickness up to $t=20$ Å (with evidence of only atomic-scale height variations).[15] At larger thickness, or at higher growth temperature, they crystallize and become structurally discontinuous (consisting of nanoclusters).[15] For the present study of the effect on conductivity of Gd and Y adatoms, we have

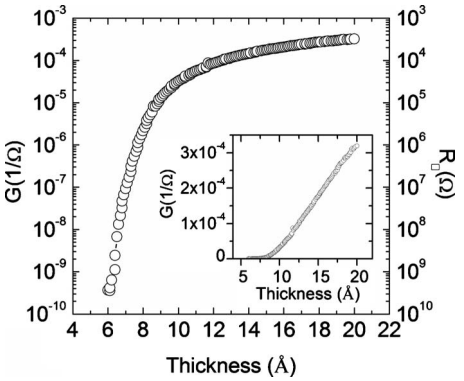

FIG. 1. 2D conductance $G=1/R_{\square}$ vs thickness t for Au deposited on thin (10 Å) Ge. In the inset the same data are shown on a linear scale. Films deposited and measured *in situ* at 8 K.

used Au films with $t \leq 20$ Å grown on 10 Å Ge, which are in the uniform regime.

Au (purity 99.999%) and Ge (purity 99.999%) were evaporated from resistively heated tungsten boats, and high purity-Gd and Y (99.999%) were evaporated from resistively heated tungsten filaments. All sources were outgassed behind a shutter before deposition. Ultrathin Au films with different thickness t (and conductance G) were grown at 8 K, and deposition was terminated at some desired G. The nominal values of t were determined using quartz crystal monitors placed in the vicinity of the substrate. The tooling factors for each source were calibrated by depositing a thick film of copper and measuring its thickness with a profilometer. The elongated geometry of the Au source gives rise to a nonsystematic error in the tooling factor. In each run we calibrated it by measuring $G(t)$ and scaling t to a fixed conductance value G_0 ($=5\times10^{-10}$ Ω^{-1}) which is the onset of measurable conductivity. For the deposition of Gd and Y, we used a deposition rate of about 0.01 Å/s, calibrated by averaging 10 min of deposition. Adatom layer thickness was controlled via deposition time. We estimate the accuracy of the Gd and Y thickness as 10–15 %.

Electrical transport was measured *in situ*. A rectangular evaporation mask (1.27 mm wide and 22.2 mm long) defined the sample geometry. Thin (100 Å) Pt contacts with narrow connections (0.25 mm wide) were prepatterned on the SiN_x substrates for current I and voltage V leads. A four-probe measurement technique was used. For all films, we ensured that I-V characteristics were ohmic. I was chosen dependent on film resistance to keep V below 1 V. The known sample geometry allowed us to calculate the sheet resistance $R_{\square}$ of the films and from that the 2D conductance $G=1/R_{\square}$. $R_{\square}(T)$ curves were recorded during repeated cooling and heating cycles (all with $T<15$ K) to ensure that no extrinsic effects such as current annealing, adsorption of residual gas molecules or oxidation of the adsorbed Gd atoms influenced the measured resistance.

Figure 1 shows the dependence of the 2D conductance G on Au thickness t (measured at 8 K during Au deposition). Measurable conduction starts at thickness of about 6 Å which corresponds to about 2 ML,[16] consistent with results in the literature.[17,18] G increases exponentially with t until, for $t>10$ Å, it crosses over to a regime where $G(t)\propto t$. This

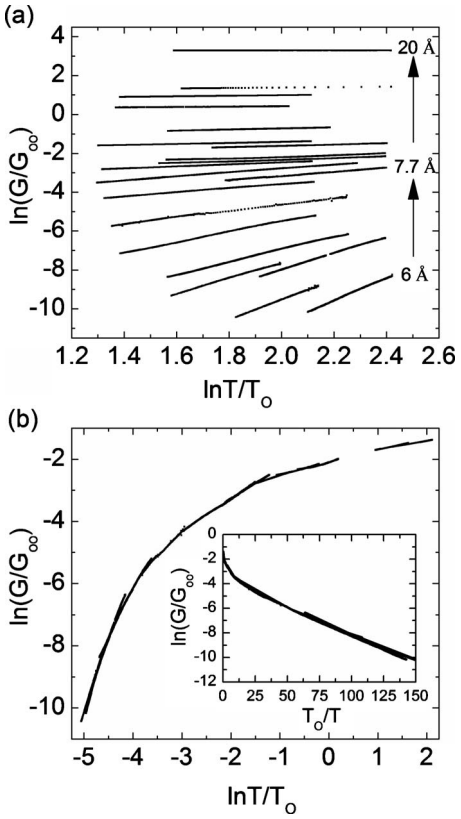

FIG. 2. (a) 2D Conductance G of Au films of different thicknesses (some are specified in the graph), grown on thin Ge vs measurement temperature T (with $T_0=1$ K) on a double logarithmic scale. Note that G is in units of fundamental conductance $G_{00}=[e^2/(2\pi^2\hbar)]=1.235\times10^{-5}$ Ω^{-1}. $R_{\square}$ of 10 Å Ge layer was unmeasurable ($R_{\square}>10$ GΩ). (b) Same data scaled by normalizing the temperature axis for each data set to fall on a single curve, as in Ref. 24. The inset shows the same data on a semilogarithmic plot of G/G_{00} versus T_0/T for the scaled curve.

crossover corresponds to the thickness (or G) value at which $k_F\ell\approx1$ (where k_F is the Fermi wavenumber and ℓ the elastic mean-free path). The exponential $G(t)$ behavior for $k_F\ell\ll1$ is commonly seen in ultrathin films, even those with Ge underlayers, and is attributed to electron tunnelling between islands.[8,12,14] This exponential $G(t)$ dependence in Fig. 1 suggests that in the ultrathin regime ($t<10$ Å), the films are made of small disconnected islands consisting of a few atoms, much smaller than for Au deposited without the Ge layer due to covalent bonding with Ge, as literature indicates.

After deposition of Au films of some desired G, we measured the temperature dependence $G(T)$ between 4 and 11 K *in situ*. The results from eighteen different Au thicknesses are shown in Fig. 2(a) where $G(T)$ is plotted in a double logarithmic scale. The films have 2D conductance between 10^{-10} and 10^{-4} Ω^{-1}. For all films, G decreases with decreasing T. For the thinnest ($t<9$ Å) films the dependence on T is exponential. For the thicker films ($t>10$ Å), it is logarithmic.

Using Au films of different $G=G_{initial}$, we evaporated Gd or Y with thicknesses between 0.1 and 2 Å (i.e., fractions of a ML, where for Gd, 1 ML=2.89 Å) and measured the resulting $G(T)$. Some examples of $G(T)$ before and after adding specified thicknesses of Gd are shown in Fig. 3. For all

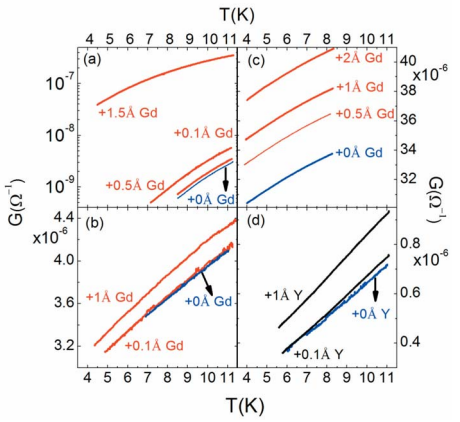

FIG. 3. (Color online) [(a)–(c)] G vs T for Au on Ge without Gd (blue lowest curves) and after adsorbing specified thicknesses of Gd (red curves). Data in (a) are in the strongly localized regime with exponential T dependence and are plotted on a semilogarithmic scale in order to display the wide range in G for Gd adsorbed on the thinnest Au film (t=6 Å). Data for (b) and (c) are closer to G_{00} (t=8.2 Å and 10 Å, respectively); data in (b) can still be fitted to Eq. (1), data in (c) not. (d) G vs T for Au (t=7.5 Å) on Ge before (blue curve) and after adsorbing specified thicknesses of Y (black curves). Measuring currents in (a) were $I=1\times10^{-9}$ A for adding 0, 0.1, and 0.5 Å of Gd and $I=50\times10^{-9}$ A for adding 1.5 Å of Gd, in (b) $I=1\times10^{-8}$ A, in (c) $I=1\times10^{-5}$ A, and in (d) $I=0.1\times10^{-7}$ A.

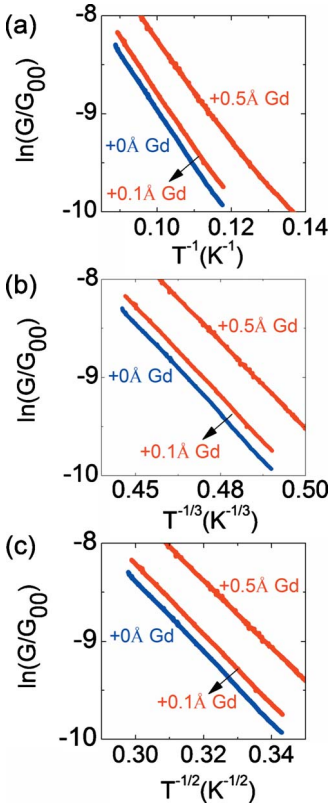

FIG. 4. (Color online) Same data as in Fig. 3(a) plotted as (a) $\ln(G/G_{00})$ versus T^{-1}, (b) versus $T^{-1/3}$, and (c) versus $T^{-1/2}$ in order to compare the data with Eq. (1).

initial conductances of the Au film prior to Gd or Y deposition ($G_{initial}$) and for all thicknesses of added Gd or Y, G increased in the temperature range measured (4 K$<T<$11 K), with no qualitative change in temperature dependence (see Figs. 3 and 4).

Figure 5 shows the conductance change ($G_{final}-G_{initial}$) of several Au films at fixed temperature (T=8 K) after adsorbing 0.1, 0.5, 1, or 2 Å of Gd versus $G_{initial}$. For comparison, we have also shown $G_{final}-G_{initial}$ after adsorbing 0.1, 0.5, 1, or 2 Å of Au instead of Gd, extracted from the thickness dependence of the Au conductance (in Fig. 1). G_{final} after adding Gd is systematically lower than G_{final} after adding Au of the same thickness, for any $G_{initial}$. To address the possible effect of magnetic disorder, we compare in Fig. 5 the results for added Gd with those for the same amount of Y, the nonmagnetic analog of Gd. There is no significant difference within the experimental error of thickness.

We discuss now our $G(T)$ data using the physics of quench-condensed ultra thin films of high electron concentration materials.[1,13,14,17] It is expected that electronic states evolve from strongly localized to weakly localized with increasing film thickness. For our films, this crossover occurs at approximately 10 Å. In the 2D limit, increasing thickness is better parameterized by increasing conductance G, which is linked to increased electron screening and decreasing disorder.

In the strong localization, low G, ultrathin film regime, the electronic wave functions are localized over a length ξ which is smaller than the inelastic scattering length ℓ_{in} of the electrons. In this regime, electrical conduction occurs through hopping of electrons between localized sites,[1] resulting in a thermally activated electrical conductance G of the form

$$G \propto \exp\left[-\left(\frac{T_0}{T}\right)^{\nu}\right], \tag{1}$$

where T_0 and ν are constants which depend on disorder, the electronic interactions, and dimensionality. For noninteracting electrons, Mott variable-range hopping is expected, leading to $\nu=1/3$ in 2D.[19] With Coulomb electron-electron interactions, the variable range hopping exponent changes to $\nu=1/2$ in any dimension.[20] In the presence of a hard gap in the density of states, electrons are expected to exhibit simple thermally activated conduction ($\nu=1$).[21]

With increasing G (thickness) and/or decreasing disorder, ξ becomes larger than ℓ_{in} (weak localization regime). In this regime, G decreases logarithmically with decreasing temperature,[17] due to quantum interference effects in 2D (Ref. 22) and disorder-enhanced Coulomb interactions between electrons.[23] The crossover between these two regimes occurs at a conductance value $G_{00}=[e^2/(2\pi^2\hbar)]\cong(80\ \mathrm{k}\Omega)^{-1}$.[17]

Our $G(T)$ data at the extremes $G\ll G_{00}$ and $G\gg G_{00}$ can be understood in terms of these theories. In accordance with the analysis of Hsu and Valles,[17] our data for the 15 thinnest films [shown in Fig. 2(b)] collapse onto a single curve by scaling T for each film as described in Ref. 24.

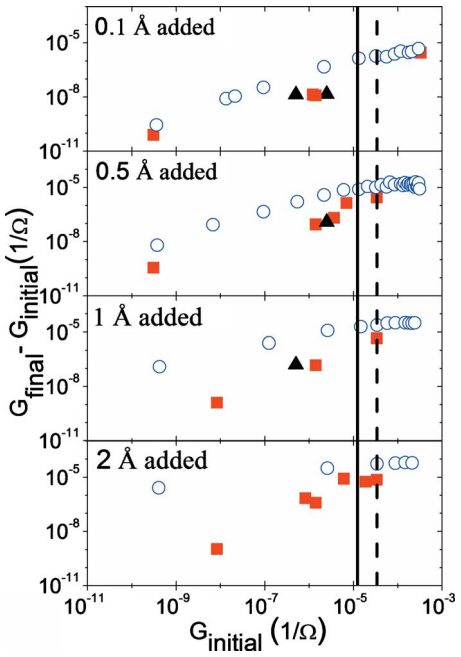

FIG. 5. (Color online) Conductance change ($G_{final}-G_{initial}$) for Au films grown and measured at 8 K before and after adding specified thicknesses of Au (blue circles), Gd (red squares), and Y (black triangles), as a function of $G_{initial}$. The thickness of the material added is indicated in each graph. The dashed line indicates the value of G, where $G(t) \propto t$. The straight line indicates G_{00}.

Most of our films fall in the regime $G \ll G_{00}$ and are therefore in the strongly localized regime. We measured only two films in the weak localization regime ($G \gg G_{00}$), where G decreases logarithmically with decreasing T as expected from weak localization theory, but we found that the slope of the curve is smaller than what is expected from theory. For the thinner films ($t<9$ Å, $G \ll G_{00}$), we found an exponential dependence and a good fit to Eq. (1). However, because of the limited temperature range, [$G(T)$ changes only by one order of magnitude], it is not possible to unambiguously distinguish between Mott variable range hopping ($\nu=1/3$) for non interacting electrons[19] and hopping with a soft ($\nu=1/2$) (Ref. 20) or hard gap ($\nu=1$) (Ref. 21) (see, for example, Fig. 4).

In order to continue the discussion of our data, we analyzed the $G(T)$ curves for our thinnest films ($G \ll G_{00}$) using Mott theory. This enables an estimate of the localization length of electrons $\xi_{Mott}=\{1/[k_B N(E_F) T_0 t]\}^{1/2}$ from T_0 (determined from the fit of the data), where k_B is the Boltzmann constant and $N(E_F)$ the density of states at the Fermi energy for 3D bulk Au. Using this approach, we find that the localization length increases with increasing film conductance from about 1.5 Å for $t=6$ Å to about 3 Å for $t \cong 8$ Å.

We now discuss the results of adding Gd and Y to the Au films. We observed an *increase* of G for all $G_{initial}$ and with all added Gd or Y (even at 1/30 ML of Gd or Y). We also found that adding Gd or Y does not change the $G(T)$ dependence, for all $G_{initial}$. For the thinnest Au film, we compared the fit to Eq. (1) (with ν kept fixed at 1/3 and 1/2) before and after adding 0.1 and 0.5 Å of Gd (see Fig. 4). We found that the prefactor is unchanged, but T_0 decreases, corresponding to an increase in the localization length. That means that the Gd is *not* inducing an increased localization of electrons. For the thicker films [Fig. 3(c)], which show conductances near G_{00}, there is no clear theory, but Gd adds conductivity without changing T dependence in all cases.

These findings are surprising because in the low conductance regime, where electrical screening of carriers is reduced, effects of added disorder are expected to be strong and the addition of scatterers such as Y or Gd is expected to *reduce* G. The results indicate however, that as material is added to the system, the effect of adding electronic states (which induces an increase in G) is larger than the effect of added potential disorder.

A measurable difference between added Au and added Gd or Y is however clear: Gd and Y always induce a smaller increase in G than Au does. Since we found that the electronic contribution mainly affect G (by more than the added potential disorder), we conclude that the difference between Au and Gd or Y is due to the different densities of available electronic states for Au and Gd/Y.

We now turn to the comparison between Gd and Y, which serves to distinguish effects coming from the Gd atoms' magnetism. We found a similar change in conductance for added Gd and Y [see Figs. 3(b), 3(d), and 5]. This means that there is either no magnetic disorder associated with the Gd ions, or that the magnetic disorder has no detectable effect on the conductivity, at least above a temperature of 5 K.

Absence of magnetic disorder could originate from the magnetic moments of the Gd ions *not* being randomly magnetically oriented, but aligned ferromagnetically, e.g., because of possible arrangement in small ferromagnetic clusters. However, we note that in the present experiment very small amount of Gd ($1/30$ ML$<t<0.7$ ML) have been used to minimize clustering effects. Moreover, Gd atoms states are most unlikely to produce a Kondo effect or hybridization of the Gd $4f$ states with Au, which would lead to absence of Gd magnetic moment, both because of the large (7/2) spin of the Gd ion and because the magnetic f states of Gd lie far below the Fermi energy.[6]

The second scenario, in which the magnetic disorder has little to no effect on the conductivity seems the most reasonable. We observe an increase in conductance and a decrease of T_0 with all added Gd or Y (even at 1/30 ML of Gd or Y). This suggests that in the strongly localized regime of conduction, the primary effect of adding Gd is to add electronic states, while effects due to localization because of disorder (potential and magnetic) are of second order.

In this case, it is likely that the larger overlap between the ionic core of Gd and the s-type electron wave functions of Au, compared with Si, results in more effective screening of both electronic potential and magnetic disorder. We finally note that after adding an overlayer of Ge (4 Å$<t<$200 Å), as was done in a previous experiment on Gd on Ge,[25] we observed no decrease in conductance.

A study of magnetoconductance of Gd deposited on quench condensed Ag films supports our interpretation.[26] In the strongly localized regime, the addition of Gd induces an increase in the system conductance at zero magnetic field (as we report here) as well as an increase in the size of the (positive) magnetoconductance to twice its original value.

These findings have been interpreted as a reduction of spin-orbit interactions and restoration of the rotational symmetry. Based on this magnetoconductance measurement, Gd shows signs of magnetic scattering, but does *not* induce electron localization at zero field, in agreement with our conclusions and observations. The authors did not measure the effects of added Y.

In summary, we have studied how magnetic Gd and nonmagnetic Y atoms influence the transport of ultrathin Au films on Ge, a highly disordered 2D system. We found that adding Gd or Y, even at fractions of a ML, leads to a very similar increase of the system conductance over a wide range of initial conductance of the 2D system with no sign of an effect of scattering centers or increased disorder due to either random electronic potentials of Gd or Y ions or magnetic disorder due to Gd spins. The increased conductance on adding Gd or Y is significantly less than the increase seen on adding similar amounts of Au, a result of different electronic states available for electron tunneling in the strong localization regime. It is likely that the intrinsically high electron concentration in Au causes an effective screening of both electronic and magnetic disorder that does not occur in Si doped with Gd. These findings indicate that magnetic disorder in strongly disordered systems has less effect in a 2D quench condensed metallic film than in a 3D strongly disordered magnetic semiconductor, which limits the realization of possible magnetoelectronic devices based on 2D metallic systems with magnetic impurities.

We would like to acknowledge very helpful discussions with R. P. Barber, G. Bergmann, R. C. Dynes, and J. M. Valles. This work was supported by NSF under NIRT Grant No. ECS-0609469 and NSF DMR.

*malemani@berkeley.edu

†Present address: Department of Physics, California State University East Bay, Hayward, California 94542, USA.

[1] P. A. Lee and T. V. Ramakrishnan, Rev. Mod. Phys. **57**, 287 (1985).

[2] S. von Molnar, A. Briggs, J. Flouquet, and G. Remenyi, Phys. Rev. Lett. **51**, 706 (1983).

[3] T. Kasuya and A. Yanase, Rev. Mod. Phys. **40**, 684 (1968).

[4] S. Von Molnar and S. Methfess, J. Appl. Phys. **38**, 959 (1967).

[5] F. Hellman, M. Q. Tran, A. E. Gebala, E. M. Wilcox, and R. C. Dynes, Phys. Rev. Lett. **77**, 4652 (1996).

[6] E. Helgren, J. J. Cherry, L. Zeng, and F. Hellman, Phys. Rev. B **71**, 113203 (2005).

[7] A. E. White, R. C. Dynes, and J. P. Garno, Phys. Rev. B **31**, 1174 (1985).

[8] S.-Y. Hsu and J. M. Valles, Phys. Rev. B **49**, 16600 (1994).

[9] H. Brune and P. Gambardella, Surf. Sci. **603**, 1812 (2009).

[10] W. L. H. Beckmann, R. Schaefer, and G. Bergmann, Europhys. Lett. **33**, 563 (1996).

[11] H. Beckmann, F. Ye, and G. Bergmann, Phys. Rev. Lett. **73**, 1715 (1994).

[12] M. Strongin, R. S. Thompson, O. F. Kammerer, and J. E. Crow, Phys. Rev. B **1**, 1078 (1970).

[13] H. White and G. Bergmann, Phys. Rev. B **40**, 11594 (1989).

[14] R. C. Dynes, J. P. Garno, and J. M. Rowell, Phys. Rev. Lett. **40**, 479 (1978).

[15] K. L. Ekinci and J. M. Valles, Phys. Rev. B **58**, 7347 (1998).

[16] The thickness of one monolayer is defined as the distance between closed packed (111) planes in the Au fcc structure; one ML is $a/\sqrt{3}=2.33$ Å, where a is the lattice constant.

[17] S.-Y. Hsu and J. M. Valles, Phys. Rev. Lett. **74**, 2331 (1995).

[18] J. J. Tu, C. C. Homes, and M. Strongin, Phys. Rev. Lett. **90**, 017402 (2003).

[19] N. F. Mott, J. Non-Cryst. Solids **1**, 1 (1968).

[20] A. L. Efros and B. I. Shklovskii, J. Phys. C **8**, L49 (1975).

[21] J. J. Kim and H. J. Lee, Phys. Rev. Lett. **70**, 2798 (1993).

[22] S. Hikami, Phys. Rev. B **24**, 2671 (1981).

[23] B. L. Altshuler, A. G. Aronov, and P. A. Lee, Phys. Rev. Lett. **44**, 1288 (1980).

[24] Y. Liu, K. A. McGreer, B. Nease, D. B. Haviland, G. Martinez, J. W. Halley, and A. M. Goldman, Phys. Rev. Lett. **67**, 2068 (1991).

[25] A. Frydman and R. C. Dynes, Phys. Rev. B **68**, 100408(R) (2003).

[26] S. Y. Hsu, Ph.D. dissertation, Brown University, 1995.